Article

Phenotypic Tracking of Antibiotic Resistance Spread via Transformation from Environment to Clinic by Reverse D₂O Single-Cell Raman Probing

Hong-Zhe Li, DanDan Zhang, Kai Yang, Xin-Li An, Qiang Pu, Shao-Min Lin, Jian-Qiang Su, and Li Cui*

Read Online

ACCESS | Metrics & More | Article Recommendations | Supporting Information

ABSTRACT: The rapid spread of antibiotic resistance threatens our fight against bacterial infections. Environments are an abundant reservoir of potentially transferable resistance to pathogens. However, the trajectory of antibiotic resistance genes (ARGs) spreading from environment to clinic and the associated risk remain poorly understood. Here, single-cell Raman spectroscopy combined with reverse D₂O labeling (Raman-rD₂O) was developed as a sensitive and rapid phenotypic tool to track the spread of plasmid-borne ARGs from soil to clinical bacteria via transformation. Based on the activity of bacteria in assimilating H to substitute prelabeled D under antibiotic treatment, Raman-rD₂O sensitively discerned a small minority of phenotypically resistant transformants from a large pool of recipient cells. Its single-cell level detection greatly facilitated the direct calculation of spread efficiency. Raman-rD₂O was further employed to study the transfer of complex soil resistant plasmids to pathogenic bacteria. Soil plasmid ARG-dependent transformability against five clinically relevant antibiotics was revealed and used to assess the spreading risk of different soil ARGs, i.e., ampicillin > cefradine and ciprofloxacin > meropenem and vancomycin. The developed single-cell phenotypic method can track the fate and risk of environmental ARGs to pathogenic bacteria and may guide developing new strategies to prevent the spread of high-risk ARGs.
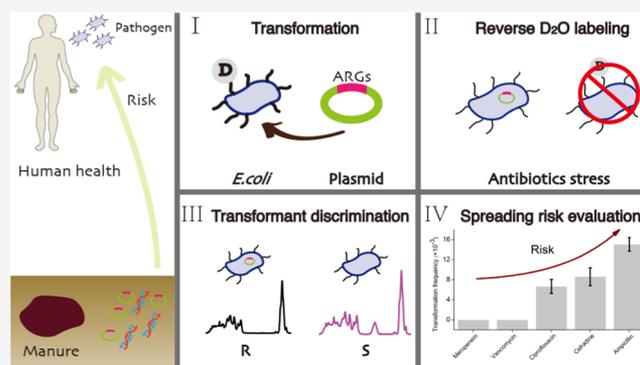

Antibiotic resistance has been posing a great threat to global public health.[1,2] More seriously, resistance continues to emerge and spread rapidly in both clinical settings and environments.[3,4] Horizontal gene transfer (HGT) contributes significantly to the rapid spread of antibiotic resistance.[5,6] HGT allows antibiotic resistance genes (ARGs) to exchange within and across a variety of microbial species and even concentrates in the same cell, driving the evolution of superbugs that are resistant to nearly all antibiotics.[7−9] Transformation, an important way of HGT, is the active uptake and recombination of extracellular DNA (eDNA) by recipient bacteria with the ability to develop competence.[10,11] eDNA comes from lysed bacteria or active secretion of bacteria and includes plasmid DNA and fragmented DNA.[12] eDNA has a high possibility of carrying diverse ARGs, including those encoding resistance to multidrugs and/or last-resort antibiotics.[13] More seriously, extracellular antibiotic resistance genes (eARGs) are frequently found on plasmids, which are mobile genetic elements and act as vehicles to mediate the spread of eARGs.[12] Moreover, more than 80 bacterial species including some pathogenic bacteria have been demonstrated to be naturally transformable.[14] These facts indicate that transformation could make a significant contribution to the spread of ARGs.

Environments have been extensively demonstrated to be reservoirs and even hotspots of ARGs, such as wastewater treatment plants, intensive animal farming, and even soils.[15−17] It is increasingly realized that environments could be abundant sources of potentially transferable resistance to pathogens, further threatening our fight against infectious disease.[18] However, the current understanding of the trajectories of ARGs from environment to clinic is very poor, such as the transformability of different environmental ARGs, hindering the development of strategies to slow down this spread. In addition, for bacteria receiving environmental ARGs, the most dangerous outcome are those expressing ARGs and displaying phenotypic antibiotic resistance, in comparison with those taking up ARGs but still phenotypically antibiotic sensitive.[19] In this respect, a functional approach to tracking down the fate of environmental eARGs and screen the recipients with phenotypic antibiotic resistance is highly demanded.
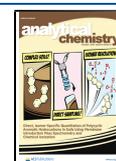
Conventional methods for the phenotypic study of natural transformation rely on cell cultivation by plating transformed cells on antibiotic-selective plates, and only those phenotypically resistant to antibiotics can grow and are regarded as transformants.[20] However, this method is very time-consuming and labor-intensive.[12] Moreover, it is limited to culturable cells, thus could be biased due to the viable but nonculturable (VBNC) state, which normally culturable bacteria can enter under different stresses.[21] It is also not applicable to more than 99% of unculturable cells in environments.[22] Reporter-gene technology is a new, rapid approach for studying HGT without the need for cultivation.[23] Green fluorescent protein reporter genes, for instance, have been used as the reporter gene to examine HGT by monitoring the change of fluorescence after uptake of plasmids by recipient cells.[24] However, because both plasmids and recipient cells need to be genetically modified, it is not applicable to real-world eDNA and bacteria.[25]

Recently, single-cell Raman spectroscopy combined with forward D_2O labeling has been developed as a rapid phenotypic tool to distinguish antibiotic-resistant (R) and sensitive (S) bacteria.[26] Microbial incorporation of D_2O induces a substitution of H by D in newly synthesized biomolecules, which can be detected as a new C−D band in a Raman spectrum.[27] Discrimination of R/S is based on the distinct C−D band intensities resulting from the different activities of R and S toward D incorporation under antibiotic treatments.[28,29] However, because both H and D can be assimilated by bacteria and H is dominantly present not only in water but also in carbon sources and amino acids, the growth rate of C−D band intensities with either incubation time or metabolic activity is low, and the short incubation time for the purpose of rapid R/S discrimination further sacrifices C−D band intensities.[27] These facts limit the discrimination sensitivity of forward D_2O labeling. By comparison, reverse D_2O labeling could improve this situation by exposing D-prelabeled cells in the medium with only H. The abundant H induces a more rapid decrease and even silence of the C−D band in metabolically active cells, compared with the slow increase of the C−D band in forward labeling.[30] Consequently, reverse D_2O single-cell Raman (Raman-rD_2O) probing could lead to more sensitive discrimination of R and S. Such high sensitivity is very important for detecting a small portion of antibiotic-resistant transformants in a large pool of recipient bacteria containing a mixture of R and S. The single-cell level evaluation of the transformation frequency overcomes the necessity of lengthy and laborious cultivation, thus facilitating the assessment of the magnitude of risks of different eARGs transferred to pathogenic bacteria.

In this study, aiming to track the spread of environmental plasmid-mediated ARGs to clinical bacteria via transformation, we developed this single-cell Raman-rD_2O approach with a high R/S discrimination sensitivity enough for reliable detection of a minority of phenotypically resistant transformants in a rapid way. The method was first verified by detecting the transformation of a known plasmid-borne ampicillin resistance gene and validated by both a cultivation-based method and polymerase chain reaction (PCR) of ampicillin resistance gene in the Raman-activated single-cell sorted transformants. It was then employed to track the spread of unknown and heterogeneous plasmid-borne ARGs extracted from soils to pathogens via transformation. Soil plasmid-dependent spread efficiencies against five important clinically relevant antibiotics were revealed and used as indicators to evaluate the spreading risks of different soil eARGs. The developed novel single-cell phenotypic method enabled rapidly tracking the fate and risk of environmental ARGs transferred to pathogenic bacteria.

EXPERIMENTAL SECTION

Bacterial Species, Antibiotics, and Growth Conditions. Bacterial species used in this study included colistin-resistant *Bacillus cereus* FIT10, ampicillin-resistant *Escherichia coli* DH5α-Amp^r that contain plasmids harboring ampicillin resistance gene (*bla*), antibiotic-sensitive *E. coli* DH5α, and competent *E. coli* JM109. Culture media used here included Luria−Bertani (LB) media (10 g of tryptone, 5 g of yeast extract, 5 g of NaCl, 1 L of H_2O) and minimal media (MM) (2 g of glucose, 0.1 g of $(NH_4)_2SO_4$, 0.06 g of KCl, 0.06 g of NaCl, 0.006 g of $MnSO_4 \cdot H_2O$, 0.006 g of $FeSO_4 \cdot 7H_2O$, 0.006 g of $MgSO_4 \cdot 7H_2O$, 200 mL of H_2O). Antibiotics used in this study included colistin (Macklin, Shanghai, China), cefradine (Macklin, Shanghai, China), and ampicillin (Solarbio, Beijing, China). They were filtrated through 0.22 μm filters (Millipore Millex) for sterilization and stored in the dark at −20 °C before use. All other chemicals without being explicitly stated were purchased from Sinopharm Chemical Reagent Co., China. All bacteria were cultured at 37 °C and 120 rpm.

Soil Plasmid Extraction. Before plasmid extraction, soil bacteria were first extracted using the Nycodenz density gradient separation method.[31] Briefly, soil samples (1 g) were mixed with 5 mL of phosphate-buffered saline (PBS) amended with 25 μL of Tween 20 and then vortexed for 30 min to detach bacteria from soil particles. To separate bacteria from soil, a soil slurry was gently added to 5 mL of Nycodenz solution (≥98%, Aladdin) at a density of 1.42 g/mL. After centrifugation at 14000*g* for 90 min, the middle layer containing bacteria was carefully extracted out and washed twice with sterile water. The obtained soil bacteria were then transferred to QIAprep Plasmid Spin Miniprep Kits (Qiagen, Germantown, MD) to extract plasmids, followed by elimination of chromosome DNA to purify the plasmid DNA. Plasmids were stored at −20 °C until further analysis.

Transformation Assay. Transformation was performed using competent *E. coli* JM109 as recipients and a pMD19-T plasmid encoding resistance to ampicillin (Takara, Beijing, China) and soil plasmids as donors. Briefly, 50 μL of *E. coli* JM109 culture was homogeneously mixed with 5 μL of pMD19-T plasmids or soil plasmids. The mixture was then incubated at 42 °C for 90 s, placed on ice for 5 min, and finally incubated in minimal medium for 4 h at 37 °C with shaking at 200 rpm.

Verification of Transformants via Cultivation-Based Method. To count the number of transformants, 100 μL of the mixture from the transformation system was spread onto LB agar selection plates containing 1× minimum inhibitory concentration (MIC) of antibiotics determined by the organizations of Clinical and Laboratory Standards Institute (CLSI).[32] The total number of bacteria was detected by spreading the properly diluted mixture onto LB agar plates without antibiotics. After incubation at 37 °C for 24 h, the colonies grown on the plates were counted. Transformation frequency was calculated as the number of transformants divided by the total number of bacteria.[33] All experiments were carried out in triplicates.

Antibiotic R/S Discrimination via Single-Cell Raman Spectroscopy with Forward and Reverse D_2O Labeling.

In forward D_2O labeling, bacteria were incubated in LB media amended with 50% (v/v) D_2O (99.8 atom % D, Aldrich) and 0.125 mg/L colistin or 2 mg/L ampicillin for different times of 0, 0.5, 1, 4, and 8 h, respectively. In reverse D_2O labeling, bacteria were first incubated in LB media amended with 50% (v/v) D_2O without antibiotics for 12 h to allow for enough D labeling and then transferred to D_2O-free media containing 0.125 mg/L colistin or 2 mg/L ampicillin for 0, 0.5, 1, 4, and 8 h. The concentrations of antibiotics used here were the MIC of antibiotic-sensitive *E. coli* DH5α (Table S1).

Verification of Transformants via Single-Cell Raman-rD$_2$O. To detect the transformants from the transformation system containing a mixture of R and S, 100 μL of the mixture was incubated in 1 mL of MM containing 50% D_2O for 2−3 h to allow for enough D labeling with a distinct C−D band. After washing twice with ultrapure water, the D-prelabeled cells were incubated in antibiotic (1× MIC)-amended D_2O-free LB media for 1 h for reverse D_2O labeling. The obtained bacteria were harvested and washed three times with ultrapure water by centrifuging at 5000 rpm for 3 min to remove the residual medium. An aliquot of 2 μL of bacterial suspension was spotted onto an aluminum foil and dried in air prior to single-cell Raman measurements. The cells without a C−D band were regarded as resistant transformants uptaking and expressing plasmid-borne ARGs, while those with an obvious C−D band were identified as sensitive cells. Spread efficiency denoting the spread risk of ARGs via transformation was determined as the number of transformants identified by Raman-rD$_2$O divided by the total number of single cells detected by Raman spectroscopy. Transformation frequency was calculated as the number of transformants divided by the proliferation rate during 1 h of incubation and the total number of cells measured by single-cell Raman spectroscopy.

The standard deviation of each measurement was calculated using the formula below

$$\text{standard deviation} = \sqrt{\frac{1}{N-1} \times \sum_{i=1}^{N} (x_i - \overline{x})^2}$$

where N is the sample size, x_i is the individual acquired transformation frequency, and $\overline{x}$ is the average number of transformation frequencies.

Single-Cell Raman Measurements. Raman spectra were acquired using a LabRAM Aramis confocal Raman microscope (Horiba Jobin-Yvon) equipped with a 300 grooves/mm diffraction grating. The type of spectral detector was an open electrode air-cooled charge-coupled device (CCD). A 532 nm Nd:YAG laser (Laser Quantum) with a 3.5 mW power was used for excitation and a 100× objective (Olympus, NA = 0.9) was used for sample observation and spectral acquisition. The acquisition time for each spectrum was 9 s. Ten to 150 individual bacteria were randomly selected for Raman measurements from each treatment. Baseline correction and normalization were preprocessed via LabSpec5 software (Horiba Jobin-Yvon). To indicate the degree of D assimilation in each bacterium, the intensities of C−H peak (2800−3100 cm^{-1}) and C−D peak (2040−2300 cm^{-1}) were used to calculate the C−D ratio of CD/(CD + CH). The standard deviation of C−D ratios in forward and reverse Raman-D_2O detection ranged from 0.006 to 0.022 (Table S5). OriginPro 8.5 was used to plot each graph. Variance analysis was performed using GraphPad Prism 5.

Raman-Activated Single-Cell Sorting and Genomic Amplification. After Raman measurements, the target bacteria of transformants were isolated using a pulse laser ejection system (HOOKE Instruments Ltd., China) one by one and collected into a receiver containing 3 μL of sterile PBS solution. The sorted cells were then lysed and subjected to whole genome amplification (WGA) via multiple displacement amplification (MDA) using the REPLI-g Single Cell Kit (Qiagen, Germany). Briefly, bacteria were lysed at 65 °C for 10 min, followed by MDA at 30 °C for 8 h and inactivation at 65 °C for 3 min. The amplified DNA products from WGA were stored at −20 °C for later use.

Genetic Investigation of *bla* Resistance Gene in Ampicillin-Resistant Transformants. To detect the presence of resistant plasmids in the transformants, *bla* genes harbored in the plasmid were amplified. PCR mixtures consisted of 1 μL of WGA product as the template, 25 μL of EX-Taq (Takara BIO, Japan), 2 μL of *bla* primer (Table S2), and 22 μL of sterilized water. The PCR program was as follows: 98 °C for 3 min for 1 cycle and 98 °C for 20 s, followed by 55 °C for 30 s for 30 cycles. PCR products of *bla* genes were visualized by agarose gel electrophoresis.

■ RESULTS AND DISCUSSION

Sensitivity of Reverse D$_2$O Single-Cell Raman Probing in Discriminating Antibiotic-Resistant and Sensitive Cells. Colistin-resistant strain *B. cereus* FIT10 and sensitive-strain *E. coli* DH5α were used as the model bacteria to ascertain the feasibility of Raman-rD$_2$O in differentiating R and S. Bacterial strains were initially incubated in D_2O-amended media to label D. These D-prelabeled bacteria were then transferred into D_2O-free media amended with 0.125 mg/L colistin for different periods of time to investigate the silencing dynamics of D. As shown in Figure 1, the C−D band of
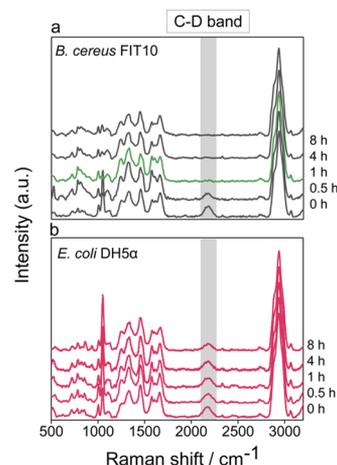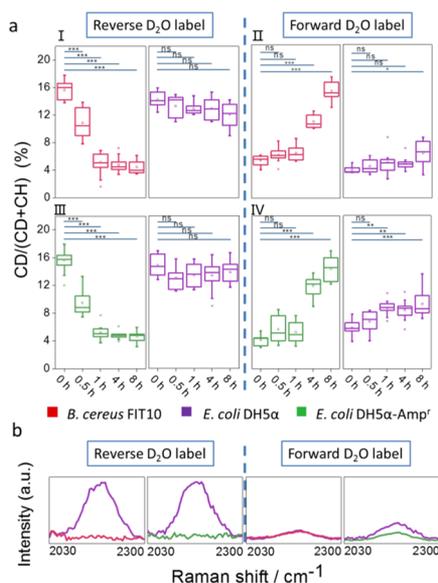

Figure 1. Time-dependent single-cell Raman spectra of D-prelabeled resistant *B. cereus* FIT10 (a) and sensitive *E. coli* DH5α (b) after incubation in LB media with 0.125 mg/L colistin for 0, 0.5, 1, 4, and 8 h, respectively.

resistant *B. cereus* FIT10 decreased rapidly and vanished completely (green spectrum) after 1 h of incubation, while the C−D band of sensitive *E. coli* DH5α was always detectable even after 8 h of incubation. The contrasting behaviors of the two bacterial strains clearly demonstrated the R/S discriminability of Raman-rD$_2$O at the phenotypic level. The reason for the silence of the C−D band was because resistant *B. cereus*

FIT10 incubated in colistin medium were still metabolically active and could rapidly assimilate H abundant in the medium to substitute D in cells during synthesizing new biomolecules such as lipid and protein.[34] By comparison, the growth and metabolic activity of antibiotic-sensitive *E. coli* DH5α were inhibited under 0.125 mg/L colistin, leading to the preservation of D in the prelabeled *E. coli* DH5α without substitution by active H assimilation.

The discrimination sensitivity of reverse D_2O labeling was further compared with the previously reported forward D_2O labeling under the same antibiotic treatment conditions.[26] Time-dependent C−D ratios (CD/(CD + CH)) of 20 individual cells in each treatment are shown in Figure 2. In

Figure 2. (a) Time-dependent C−D ratios of colistin-resistant *B. cereus*, ampicillin-resistant *E. coli* DH5α-Amp^r, and sensitive *E. coli* DH5α in reverse (I, III) and forward D_2O labeling (II, IV). (b) Single-cell C−D Raman spectra of the three bacterial strains in reverse and forward D_2O labeling after 1 h of incubation with 1× MIC of antibiotics.

reverse D_2O labeling, C−D ratios of D-prelabeled colistin-resistant *B. cereus* FIT10 cells treated with colistin dropped rapidly and significantly with time from 16 to 5% after only 1 h of incubation, while in forward D_2O labeling after the same 1 h, no significant increase was observed (Figure 2a, patterns I and II). This result agreed with our prediction that the large amount of H in the medium dominant over D can induce a more dramatic replacement of D by H in reverse labeling than H by D in forward labeling. For antibiotic-sensitive *E. coli* DH5α (Figure 2a, patterns I and II), C−D ratios were kept the same with time either at a high level in reverse labeling or a very low level in forward labeling. In terms of the sensitivity and rapidness in differentiating R and S, C−D bands after a short 1 h of incubation in reverse and forward D_2O labeling were compared in Figure 2b. The difference of C−D ratios in R and S was much more prominent in reverse labeling than in forward labeling, wherein no significant difference was observed in R and S.

In addition to colistin that is a last-line antibiotic used to treat multidrug-resistant Gram-negative bacteria by disrupting bacterial membranes and causing cytoplasmic leakage,[35] a first-line antibiotic of ampicillin with a different action mechanism

of inhibiting the synthesis of the cell wall was also tested on ampicillin-resistant *E. coli* DH5α-Amp^r and sensitive *E. coli* DH5α. The results shown in Figure 2a (patterns III and IV) and Figure 2b were very similar to those of colistin treatment, clearly demonstrating that reverse D_2O labeling was more sensitive in R/S differentiation than forward labeling and applicable to antibiotics of different action mechanisms. Moreover, the silence of the C−D band was observed in both types of resistant cells after 1 h of antibiotic treatment, demonstrating that it can be used as a sensitive and highly visualized biomarker to distinguish R and S at the phenotypic level. To be more quantitatively explicit, we defined C−D ratios less than 6.4% as the silence of the C−D band or the resistance cutoff value. It was determined by calculating the mean + 3 × standard deviation of C−D ratios in *E. coli* DH5α incubated without D_2O (Figure S1).

Utility of Raman-rD$_2$O in Revealing Horizontal Transfer of ARGs via Transformation. Single-cell Raman-rD$_2$O was then used to study HGT of ARGs via transformation. HGT is a highly heterogeneous process where only a small population of recipient cells uptake donor eARGs and become phenotypically resistant to antibiotics. The highly sensitive Raman-rD$_2$O in differentiating R and S facilitated the identification of resistant transformants from recipient cells. Scheme 1 shows the workflow of detecting transformation by

Scheme 1. Workflow for Transformation Testing via Single-Cell Raman-rD$_2$O
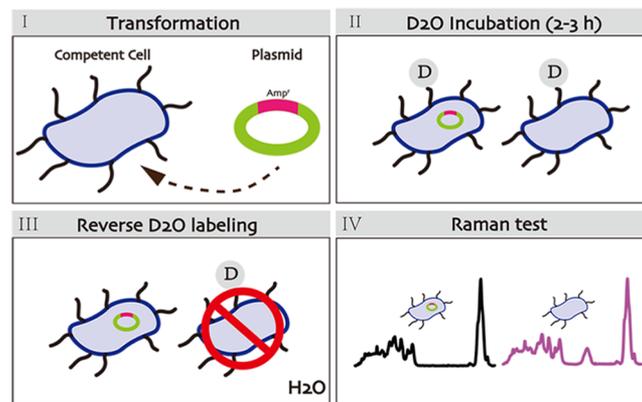
Raman-rD$_2$O. Plasmid-borne *bla* genes encoding resistance to ampicillin were used as the donor eARGs and competent *E. coli* JM109 were used as the recipient cells.[21,26] *E. coli* JM109 were mixed with plasmids gently to allow for transformation to occur. All of the resulting cells with or without plasmids were incubated in D_2O-amended media to produce a distinct C−D band (Figure S2). The D-prelabeled cells were then incubated in 1× CLSI MIC (32 μg/mL) of ampicillin-amended media (without D_2O) for 1 h to substitute D with H, followed by single-cell Raman measurement. The time of 1 h was enough to silence the C−D band in resistant cells and enable differentiation of phenotypically resistant transformants from sensitive cells. Meanwhile, antibiotic-resistant *E. coli* DH5α-Amp^r and sensitive *E. coli* DH5α used as controls were subjected to the same workflow in II−IV. Figure 3a shows the C−D ratios of three types of bacteria before (0 h) and after 1 h of reverse D_2O labeling under ampicillin treatment. Each point represents a measurement of a single bacterium. All of these bacteria at 0 h showed an obvious C−D band with a C−D
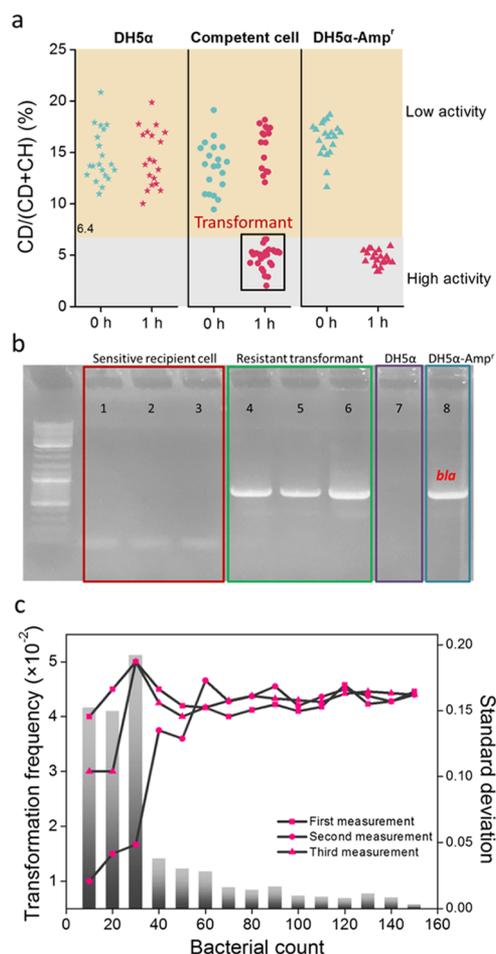
Figure 3. (a) C−D ratios of D-prelabeled *E. coli* DH5α (sensitive control), *E. coli* DH5α-Amp[r] (resistant control), and recipient competent *E. coli* transformed with *bla* plasmids after 1 h of incubation in ampicillin-amended LB media detected by Raman-rD$_2$O. Each dot is a Raman measurement of a single cell. The C−D ratios below the threshold of 6.4% determined by the mean + 3 standard deviation of C−D ratios of cells without incubation with D$_2$O indicate the resistant transformants without D labeling. (b) Electrophoresis of the PCR product of the plasmid-borne *bla* gene. Lane 1−3: sensitive recipient cells with high C−D ratios, lane 4−6: resistant transformants with <10% C−D ratios, lane 7: *E. coli* DH5α without plasmid, and lane 8: *E. coli* DH5α-Amp[r] with *bla* plasmid. (c) Transformation frequencies (line) and standard deviation of transformation frequencies of the plasmid-borne *bla* gene (column) against the number of single cells measured by single-cell Raman-rD$_2$O.

ratio higher than 9%. After 1 h of incubation, *E. coli* DH5α (sensitive control) still held high C−D ratios, indicating its low activity toward H assimilation under ampicillin treatment. By comparison, C−D ratios in all *E. coli* DH5α-Amp[r] (resistant control) dropped to below 6.4%, indicating its high metabolic activity in assimilating H from the medium to replace the prelabeled D. Different from the results of sensitive and resistant controls, C−D ratios from competent cells after plasmid transformation spanned a broad range from 0 to 20%, covering both high and low activities, indicating the coexistence of resistant and sensitive cells after transformation. The subpopulation with high activities and thus low C−D ratios (<6.4%) close to those of resistant control were regarded as phenotypically resistant transformants uptaking plasmids,

while those with high C−D ratios similar to those of sensitive control were regarded as sensitive recipient cells.

To confirm the presence of resistant plasmids in the transformants identified by Raman-rD$_2$O, an individual bacterium with or without the C−D band after plasmid transformation was sorted out through the single-cell laser ejection system. The nearly nondestructive nature of Raman detection allows for single-cell sorting and downstream genotypic analysis.[19,36] The sorted single cells were subjected to single-cell whole genome amplification, followed by PCR amplification of *bla* gene on plasmids and visualization on an agarose gel (Figure 3b). The bright bands of *bla* genes were observed in both the transformants and resistant control of *E. coli* DH5α-Amp[r], indicating the presence of plasmids, while no band was found in the sensitive recipient cells and sensitive control of *E. coli* DH5α, indicating the lack of plasmids. These results fully verified that the phenotypically resistant transformants identified by Raman-rD$_2$O indeed acquired the extracellular resistant plasmids via transformation, confirming the reliability of this method.

Transformation frequency is an important parameter to assess the risk and contribution of HGT in spreading antibiotic resistance. The single-cell level detection of Raman-rD$_2$O provided a rapid means to calculate the transformation frequency without the necessity of lengthy and laborious plating and colony enumeration. Using the workflow shown in Scheme 1, the resistant transformants were found to proliferate by around 10-fold (Table S3) during 1 h of incubation in the antibiotic-amended D$_2$O-free medium (Scheme 1, III), while the growth of sensitive cells was inhibited by antibiotics. Therefore, the 10-fold increase of the number of transformants should be corrected, and transformation frequency was calculated as the number of transformants (C−D ratios below 6.4%) divided by 10 and the total number of cells measured by single-cell Raman spectroscopy. To find a proper cell number leading to an accurate calculation of transformation frequency, a total of 450 cells in triplicate (150 cells for each repetition) were randomly measured by single-cell Raman spectroscopy. When the number of cells was less than 40, the transformation frequency varied greatly either in each measurement or across the three replicates (Figure 3c), indicating that this number was too small to provide a reliable frequency. With the number increasing, the transformation frequency gradually stabilized in all three measurements and reached a stable value of 4.33 × 10^{-2} (Figure 3c). Hence, 40 was set as the least number of cells required to obtain an accurate frequency. We noticed that this frequency value was close to the transformation frequency of 5.07 × 10^{-2} derived from the conventional plate culturing experiment (Table S4), demonstrating that single-cell Raman-rD$_2$O was a reliable approach for estimating the transformability.

Evaluation of the Transformability of Diverse Environmental Plasmid-Mediated eARGs to Pathogen via Single-Cell Raman-rD$_2$O. Environments are a reservoir of ARGs.[37] Arable soils, especially those receiving manure organic fertilizers, have been found to contain highly abundant and diverse ARGs encoding resistance to nearly all types of antibiotics.[37] Some soil ARGs were abundantly found in mobile genetic elements such as plasmids, raising the possibility of HGT.[38] Moreover, soil ARGs were demonstrated to transport to plants grown on the soils including those ready-to-eat foods, raising a health risk of spreading ARGs from soils to a human pathogen.[3] Although numerous studies have

investigated ARG-harboring plasmids in environments,[39,40] their transmission ability and risk to human pathogens were rarely investigated. Here, single-cell Raman-rD$_2$O was used as a phenotypic tool to study the transformation from a mixture of plasmid-borne ARGs extracted from soils to *E. coli*, a typical human pathogen.

To comprehensively assess the transmission of soil eARGs, five most concerned antibiotics within the World Health Organization (WHO) antibiotic-resistant "priority pathogen" lists, including meropenem, vancomycin, ampicillin, cefradine, and ciprofloxacin, were used to discern each type of transformant.[41] Transformation was performed following Scheme 1 by mixing plasmids extracted from soils with recipient *E. coli* and applying the above five antibiotics in the D removal step. A total of around 150 single-cell Raman spectra after transformation were acquired from each antibiotic treatment. As shown in Figure 4a, high C−D ratios were
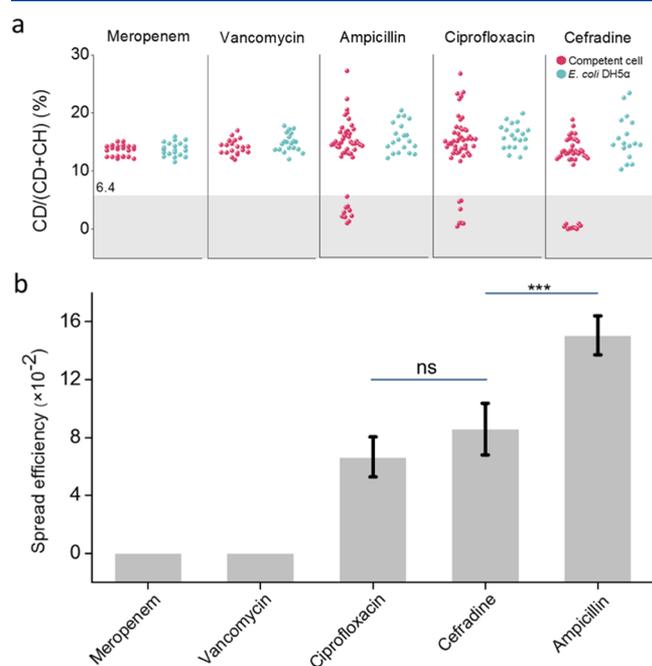
Figure 4. (a) C−D ratios of *E. coli* DH5α (sensitive control) and D-prelabeled recipient competent *E. coli* transformed with soil plasmid-borne ARGs after 1 h of incubation in LB media amended with meropenem, vancomycin, ampicillin, ciprofloxacin, and cefradine, respectively. Each dot is a Raman measurement of a single cell. The C−D ratios below the threshold of 6.4% indicate the resistant transformants without D labeling. (b) Spread efficiencies of soil plasmid-borne ARGs encoding resistance to meropenem, vancomycin, ciprofloxacin, cefradine, and ampicillin. Comparisons denoted by asterisks were statistically significant (one-way analysis of variance (ANOVA), *P* < 0.001).

observed in *E. coli* DH5α (sensitive control) in all five antibiotics, indicating that their metabolic activities were effectively inhibited by antibiotics. By comparison, C−D ratios of recipient *E. coli* after transformation displayed different profiles against each antibiotic. A small population in response to ampicillin, ciprofloxacin, and cefradine displayed silent C−D bands (C−D ratios < 6.4%), indicating that soil eARGs encoding resistance to these three antibiotics were successfully transformed and expressed by recipient cells. In contrast, no silent C−D band was observed in meropenem and vancomycin, indicating that these two antibiotic-associated

soil plasmid-borne ARGs lacked transformability. Although the type and abundance of soil plasmids harboring different ARGs were still a black box, single-cell Raman-rD$_2$O clearly illustrated the soil plasmid-dependent eARG transformation capability.

Different plasmids have been demonstrated to have different fitness costs that affect the proliferation characteristics of bacteria.[42] Because the plasmids extracted from soil were very diverse, and different resistant plasmids may encode the same phenotypic resistance, such complexity made it impossible to correct the transformation frequency specific for each strain using the same means as for the known plasmid. A better way to illustrate the transformability of plasmids is needed. Considering that the overall spreading ability of plasmid-borne ARGs by transformation depends on both the transformation frequency and the proliferation of transformants afterward, the concept of "spread efficiency", given as the ratio of transformants (number of cells without the C−D band) to recipients (all cells measured by Raman spectroscopy) after incubation, was used to represent the spread risk.

The more the spread efficiency of ARGs, the greater the risk of dissemination. As shown in Figure 4b, the spread efficiencies for the five antibiotics were 1.5×10^{-1} (ampicillin), 8.6×10^{-2} (cefradine), 6.7×10^{-2} (ciprofloxacin), and 0 (meropenem and vancomycin), indicating the spreading risk of soil eARGs in the order of ampicillin > cefradine and ciprofloxacin > meropenem and vancomycin. Considering that cefradine (cephalosporin)/ciprofloxacin (fluoroquinolone)- and ampicillin (β-lactams)-resistant pathogens have been categorized as high and medium priority in WHO priority pathogen list, respectively, the transformation of soil eARGs against these antibiotics in *E. coli* indicated a high health risk. Fortunately, soil eARGs conferring resistance to meropenem and vancomycin that were associated with pathogens classified as critical and high priority in WHO lists were not transferred to *E. coli*. The different spread efficiencies could be related to the original abundance of soil plasmids carrying different types of eARGs, the size of plasmids that is less favorable for transformation at a larger size, the host range, and the fitness cost of plasmids.[43]

Conventional plate culturing was also used to determine the transformation frequency, and it was interesting to find the same trend as that of Raman-rD$_2$O, i.e., ampicillin (1.9×10^{-3}) > ciprofloxacin (5.9×10^{-4}) and cefradine (8.8×10^{-4}) > meropenem and vancomycin (0) (Figure S3). After a careful interrogation, the frequencies determined by plate culturing were 80−110-fold lower than the spread efficiencies determined by Raman-rD$_2$O. Cultivation methods have been frequently indicated to potentially underestimate the extent of plasmid HGT[22] because bacteria carrying resistant plasmids could enter a VBNC state under some stressful conditions despite resistant plasmids being able to stably reside. In addition, fitness costs imposed by some plasmid acquisition and expression were demonstrated to slow microbial growth by a large extent of 1000-fold.[44] The presence of none or slow-growing cells that cannot grow to a colony induced the underestimation of plasmid-containing bacteria. By comparison, single-cell Raman-rD$_2$O is an activity-based culture-independent method. Its advantage over the growth-based method has been clearly indicated to be its capability of detecting nongrowing but metabolically active cells, such as growth-inhibited cells by antibiotics and ultraviolet (UV)-injured but viable bacteria.[21,26,28] Therefore, single-cell Raman-

rD$_2$O overcomes the problem of underestimation caused by the presence of none or slow-growing cells carrying plasmids. In addition, the lengthy cultivation of at least overnight in an antibiotic-selective medium increases the possibility of spontaneous mutations of recipients.[45] By comparison, the as short as 1 h of incubation in antibiotic-amended medium required by Raman-rD$_2$O dramatically reduced the mutation possibility. As such, single-cell Raman-rD$_2$O provides a reliable and rapid phenotypic method to investigate the transformation of eARGs from environment to clinic and the associated dissemination risk of different types of eARGs.

CONCLUSIONS

This is the first demonstration that single-cell Raman spectroscopy combined with reverse D$_2$O labeling can phenotypically track the spread of antibiotic resistance from environment to clinic via transformation in a reliable and rapid way. Single-cell Raman-rD$_2$O was demonstrated to be highly sensitive and rapid (after only 1 h of incubation) in discriminating phenotypically resistant bacteria based on the finding that D in active cells can be rapidly substituted by H predominantly in an antibiotic-amended medium. The resulting rapid silence of the C−D band was established as a sharp indicator of phenotypic resistance. In employing it to study the transformation of plasmid-borne ARGs to bacteria, Raman-rD$_2$O clearly discerned the small population of resistant transformants from a large pool of recipient cells. The single-cell level detection enabled the direct calculation of spread efficiencies without the lengthy cultivation. Single-cell Raman-rD$_2$O was further employed to assess the transformability of complex soil plasmid-borne ARGs to pathogenic bacteria. Soil plasmid ARG-dependent spread efficiencies against five clinically relevant antibiotics were revealed, illustrating their different spreading risks via transformation.

This new phenotypic method helps shed light on the trajectories of the spread of ARGs from environment to clinic and reveal their potential risk. In the future, Raman-rD$_2$O can be applied to decipher the factors that affect the successful transfer and persistence of resistant plasmids. As a phenotype method, it can also be linked with genotype investigation to advance our understanding of the spreading risk of environmental plastidome. It also offers a potential way for other HGT processes, such as transconjugation and transduction. These studies promote us to develop strategies to slow down and prevent the spread of high-risk environmental eARGs to clinics.

ASSOCIATED CONTENT

Ⓢ Supporting Information

The Supporting Information is available free of charge at https://pubs.acs.org/doi/10.1021/acs.analchem.0c03218.

MIC of antibiotics for different bacteria; PCR primers of *bla* gene; proliferation rate of *E. coli* DH5α-Amp^r; transformation frequency of plasmid-borne gene; standard deviation of C−D ratios; and C−D ratios of *E. coli* DH5α in media with and without D$_2$O (PDF)

AUTHOR INFORMATION

Corresponding Author

Li Cui − *Key Lab of Urban Environment and Health, Institute of Urban Environment, Chinese Academy of Sciences, Xiamen 361021, China;* orcid.org/0000-0002-0708-8899; Phone: 86-5926190780; Email: lcui@iue.ac.cn

Authors

Hong-Zhe Li − *Key Lab of Urban Environment and Health, Institute of Urban Environment, Chinese Academy of Sciences, Xiamen 361021, China; University of Chinese Academy of Sciences, Beijing 100049, China*

DanDan Zhang − *Key Lab of Urban Environment and Health, Institute of Urban Environment, Chinese Academy of Sciences, Xiamen 361021, China*

Kai Yang − *Key Lab of Urban Environment and Health, Institute of Urban Environment, Chinese Academy of Sciences, Xiamen 361021, China; University of Chinese Academy of Sciences, Beijing 100049, China;* orcid.org/0000-0002-3554-3334

Xin-Li An − *Key Lab of Urban Environment and Health, Institute of Urban Environment, Chinese Academy of Sciences, Xiamen 361021, China*

Qiang Pu − *Key Lab of Urban Environment and Health, Institute of Urban Environment, Chinese Academy of Sciences, Xiamen 361021, China; University of Chinese Academy of Sciences, Beijing 100049, China*

Shao-Min Lin − *Key Lab of Urban Environment and Health, Institute of Urban Environment, Chinese Academy of Sciences, Xiamen 361021, China; College of Life Sciences, Fujian Agriculture and Forestry University, Fuzhou 350002, China*

Jian-Qiang Su − *Key Lab of Urban Environment and Health, Institute of Urban Environment, Chinese Academy of Sciences, Xiamen 361021, China;* orcid.org/0000-0003-1875-249X

Complete contact information is available at:
https://pubs.acs.org/10.1021/acs.analchem.0c03218

Notes

The authors declare no competing financial interest.

REFERENCES

(1) Zhu, Y. G.; Gillings, M.; Simonet, P.; Stekel, D.; Banwart, S.; Penuelas, J. *Science* **2017**, *357*, 1099−1100.

(2) Zhu, Y. G.; Gillings, M.; Simonet, P.; Stekel, D.; Banwart, S.; Penuelas, J. *Global Change Biol.* **2018**, *24*, 1488−1499.

(3) Allen, H. K.; Donato, J.; Wang, H. H.; Cloud-Hansen, K. A.; Davies, J.; Handelsman, J. *Nat. Rev. Microbiol.* **2010**, *8*, 251−259.

(4) Baquero, F.; Martinez, J. L.; Canton, R. *Curr. Opin. Biotechnol.* **2008**, *19*, 260−265.

(5) Stalder, T.; Press, M. O.; Sullivan, S.; Liachko, I.; Top, E. M. *ISME J.* **2019**, *13*, 2437−2446.

(6) Thomas, C. M.; Nielsen, K. M. *Nat. Rev. Microbiol.* **2005**, *3*, 711−721.

(7) Ochman, H.; Lawrence, J. G.; Groisman, E. A. *Nature* **2000**, *405*, 299−304.

(8) Adegoke, A. A.; Faleye, A. C.; Singh, G.; Stenstroem, T. A. *Molecules* **2017**, *22*, No. 29.

(9) Aboderin, A. O.; Al-Abri, S. S.; Jalil, N. A.; Benzonana, N.; Bhattacharya, S.; Brink, A. J.; Burkert, F. R.; Cars, O.; Cornaglia, G.; Dyar, O. J.; et al. *Lancet Infect. Dis.* **2018**, *18*, 318−327.

(10) Levy-Booth, D. J.; Campbell, R. G.; Gulden, R. H.; Hart, M. M.; Powell, J. R.; Klironomos, J. N.; Pauls, K. P.; Swanton, C. J.; Trevors, J. T.; Dunfield, K. E. *Soil Biol. Biochem.* **2007**, *39*, 2977−2991.

(11) Mao, D. Q.; Luo, Y.; Mathieu, J.; Wang, Q.; Feng, L.; Mu, Q. H.; Feng, C. Y.; Alvarez, P. J. J. *Environ. Sci. Technol.* **2014**, *48*, 71−78.

(12) Goetsch, H. E.; Love, N. G.; Wigginton, K. R. *Environ. Sci. Technol.* **2020**, *54*, 1808−1815.

(13) Dong, P.; Wang, H.; Fang, T.; Wang, Y.; Ye, Q. *Environ. Int.* **2019**, *125*, 90−96.

(14) Oliveira, P. H.; Touchon, M.; Cury, J.; Rocha, E. P. C. *Nat. Commun.* **2017**, *8*, No. 841.

(15) Zhu, Y. G.; Johnson, T. A.; Su, J. Q.; Qiao, M.; Guo, G. X.; Stedtfeld, R. D.; Hashsham, S. A.; Tiedje, J. M. *Proc. Natl. Acad. Sci. U.S.A.* **2013**, *110*, 3435−3440.

(16) Cacace, D.; Fatta-Kassinos, D.; Manaia, C. M.; Cytryn, E.; Kreuzinger, N.; Rizzo, L.; Karaolia, P.; Schwartz, T.; Alexander, J.; Merlin, C.; Garelick, H.; Schmitt, H.; de Vries, D.; Schwermer, C. U.; Meric, S.; Ozkal, C. B.; Pons, M.-N.; Kneis, D.; Berendonk, T. U. *Water Res.* **2019**, *162*, 320−330.

(17) Forsberg, K. J.; Patel, S.; Gibson, M. K.; Lauber, C. L.; Knight, R.; Fierer, N.; Dantas, G. *Nature* **2014**, *509*, 612−616.

(18) Wright, G. D. *Curr. Opin. Microbiol.* **2010**, *13*, 589−594.

(19) Wang, Y.; Xu, J. B.; Kong, L. C.; Li, B.; Li, H.; Huang, W. E.; Zheng, C. M. *Environ. Microbiol.* **2020**, *22*, 2613−2624.

(20) Santala, V.; Karp, M.; Santala, S. *FEMS Microbiol. Lett.* **2016**, *363*, No. fnw125.

(21) Zhang, S. H.; Guo, L. Z.; Yang, K.; Zhang, Y.; Ye, C. S.; Chen, S.; Yu, X.; Huang, W. E.; Cui, L. *Front. Microbiol.* **2018**, *9*, No. 2243.

(22) Sørensen, S. J.; Bailey, M.; Hansen, L. H.; Kroer, N.; Wuertz, S. *Nat. Rev. Microbiol.* **2005**, *3*, 700−710.

(23) Zhang, J.; Campbell, R. E.; Ting, A. Y.; Tsien, R. Y. *Nat. Rev. Mol. Cell Biol.* **2002**, *3*, 906−918.

(24) Aminov, R. I. *Front. Microbiol.* **2011**, *2*, No. 158.

(25) Tsien, R. Y. *Annu. Rev. Biochem.* **1998**, *67*, 509−544.

(26) Yang, K.; Li, H. Z.; Zhu, X.; Su, J. Q.; Ren, B.; Zhu, Y. G.; Cui, L. *Anal. Chem.* **2019**, *91*, 6296−6303.

(27) Berry, D.; Mader, E.; Lee, T. K.; Woebken, D.; Wang, Y.; Zhu, D.; Palatinszky, M.; Schintlmeister, A.; Schmid, M. C.; Hanson, B. T.; et al. *Proc. Natl. Acad. Sci. U.S.A.* **2015**, *112*, E194−E203.

(28) Tao, Y. F.; Wang, Y.; Huang, S.; Zhu, P. F.; Huang, W. E.; Ling, J. Q.; Xu, J. *Anal. Chem.* **2017**, *89*, 4108−4115.

(29) Ueno, H.; Kato, Y.; Tabata, K. V.; Noji, H. *Anal. Chem.* **2019**, *91*, 15171−15178.

(30) Wang, Y.; Song, Y. Z.; Tao, Y. F.; Muhamadali, H.; Goodacre, R.; Zhou, N. Y.; Preston, G. M.; Xu, J.; Huang, W. E. *Anal. Chem.* **2016**, *88*, 9443−9450.

(31) Eichorst, S. A.; Florian, S.; Tanja, W.; Arno, S.; Michael, W.; Dagmar, W. *FEMS Microbiol. Ecol.* **2015**, *91*, No. fiv106.

(32) Patel, J. B.; Cockerill, F. R.; Bradford, P. A. *Clin. Lab. Stand. Inst.* **2015**, *35*, 29−50.

(33) Antoci, V.; Adams, C. S.; Parvizi, J.; Davidson, H. M.; Composto, R. J.; Freeman, T. A.; Wickstrom, E.; Ducheyne, P.; Jungkind, D.; Shapiro, I. M.; Hickok, N. J. *Biomaterials* **2008**, *29*, 4684−4690.

(34) Zhang, X. N.; Gillespie, A. L.; Sessions, A. L. *Proc. Natl. Acad. Sci. U.S.A.* **2009**, *106*, 12580−12586.

(35) Partridge, D. G. *J. Infect.* **2009**, *59*, 376.

(36) Jing, X.; Gou, H.; Gong, Y.; Su, X.; Xu, L.; Ji, Y.; Song, Y.; Thompson, I. P.; Xu, J.; Huang, W. E. *Environ. Microbiol.* **2018**, *20*, 2241−2255.

(37) Qiao, M.; Ying, G. G.; Singer, A. C.; Zhu, Y. G. *Environ. Int.* **2018**, *110*, 160−172.

(38) Rodríguez-Beltrán, J.; Vidar, S.; Macarena, T. R.; Carmen, V.; Rafael, P. M.; Alvaro, S. M. *Proc. Natl. Acad. Sci. U.S.A.* **2020**, *117*, 15755−15762.

(39) Lu, W.; Wang, M.; Wu, J. Q.; Jiang, Q. Y.; Jin, J. R.; Jin, Q.; Yang, W. W.; Chen, J.; Wang, Y. J.; Xiao, M. *Environ. Pollut.* **2020**, *260*, No. 113998.

(40) Fan, X. T.; Li, H.; Chen, Q. L.; Zhang, Y. S.; Ye, J.; Zhu, Y. G.; Su, J. Q. *Front. Microbiol.* **2019**, *10*, No. 194.

(41) Shrivastava, S. R.; Shrivastava, P. S.; Ramasamy, J. *J. Med. Soc.* **2018**, *32*, 76.

(42) Andersson, D. I.; Levin, B. R. *Curr. Opin. Microbiol.* **1999**, *2*, 489−493.

(43) Pifer, M. L.; Smith, H. O. *Proc. Natl. Acad. Sci. U.S.A* **1985**, *82*, 3731−3735.

(44) Yang, Q.; Li, M.; Spiller, O. B.; Andrey, D. O.; Hinchliffe, P.; Li, H.; MacLean, C.; Niumsup, P.; Powell, L.; Pritchard, M.; Papkou, A.; Shen, Y.; Portal, E.; Sands, K.; Spencer, J.; Tansawai, U.; Thomas, D.; Wang, S. L.; Wang, Y.; Shen, J. Z.; et al. *Nat. Commun.* **2017**, *8*, No. 2054.

(45) Jin, M.; Liu, L.; Wang, D. N.; Yang, D.; Liu, W. L.; Yin, J.; Yang, Z. W.; Wang, H. R.; Qiu, Z. G.; Shen, Z. Q.; Shi, D. Y.; Li, H. B.; Guo, J. H.; Li, J. W. *ISME J.* **2020**, *14*, 1847−1856.